ESRF	**Experiment title:** Structure elucidation of microcrystals in the system Mn/Bi/Te and substitution variants thereof	**Experiment number**: CH-5142
Beamline: ID11	**Date of experiment**: from: 08.02.2018 to: 13.02.2018	**Date of report**: 18.12.2018
Shifts: 12	**Local contact(s)**: Jonathan Wright	*Received at ESRF:*

Names and affiliations of applicants (* indicates experimentalists):

Prof. Dr. Oliver Oeckler* (Leipzig University, Munich)

M. Sc. Markus Nentwig (Leipzig University)

Dr. Christopher Benndorf* (Leipzig University)

M. Sc. Tobias Stollenwerk* (Leipzig University)

M. Sc. Lucien Eisenburger* (Ludwig Maximilian University, Munich)

M. Sc. Daniel Günther* (Leipzig University)

Report:

Note that some samples investigated during this beamtime correspond to project CH5140, whereas some samples from CH5142 were investigated during beamtime CH5140

Aim

Manganese bismuth tellurides are a new class of potential topological insulators that contain magnetic transition metal ions and may also possess intriguing thermoelectric properties.[1,2,3] In the pseudo-binary system MnTe-Bi_2Te_3, only the structure of $MnBi_2Te_4$ has been determined from powder data so far.[4] It crystallizes in the layered $GeSb_2Te_4$ structure type with disordered cations. One aim of this project was the precise crystal structure determination of related compounds in the system Mn/Bi/Te, e.g., $MnBi_6Te_{10}$. $MnBi_2Te_4$, and probably also the other new phases, are metastable at room temperature and start decomposing into the binary compounds Bi_2Te_3 and manganese tellurides at ~150 °C.[4] These layered structures often tend to form extremely thin platelet-shaped crystals. Thus, structure determination by conventional single crystal X-ray diffraction is not successful. Due to the large *c* lattice parameters of these compounds, powder X-ray diffraction is impeded as well. Crystallites in microcrystalline samples were identified and characterized by transmission electron microscopy (TEM) and EDX spectroscopy. These crystallites were then investigated on the TEM grids by means of micofocussed synchrotron radiation.[5,6]

In a broader perspective, functional materials consisting of non-toxic, earth-abundant and affordable elements gain more and more interest. Therefore, copper, iron and sulfur seem highly attractive for thermoelectric applications. Cu_5FeS_4, known as the mineral bornite, is captivating because of its polymorphism and its mixed valence states. Mößbauer data indicate the existence of low-spin Fe^{2+} next to high-spin Fe^{3+} in Cu_5FeS_4 at room temperature.[7] Substitution of S by Se with higher Se contents than in literature [8] could enable the stabilization of new polymorphs in $Cu_5FeS_{4-x}Se_x$ or in Cu-deficient phases and the characterization of their thermoelectric properties in conjunction with their electronic structure at higher temperatures. High-resolution temperature-dependent powder X-ray diffraction (PXRD) is necessary to determine the temperature ranges where the unknown superstructure and its high-temperature polymorphs are stable. Room-temperature PXRD of metastable $Cu_4FeS_{2.2}Se_{1.6}$ shows some broad reflections that

transform to a known polymorph upon slow cooling, and some side phase is formed. Temperature-dependent PXRD reveals the temperature ranges where the metastable compound can exist. In the system Cu/Bi/Se, „$CuBi_3Se_5$“ crystallizes in the space-group $C2/m$.[9] The appropriate sum formula is $Cu_{1.78}Bi_{4.73}Se_8$,[9] which shows a flexibility towards non-stoichiometry that involves disordered interstitial Cu atoms.[10,11,12] Only few substitution variants have been reported, e.g. $Cu_{1.6915}In_{0.0085}Bi_{4.7}Se_8$.[13] Their thermoelectric properties are of great interest because according to the PLEC (phonon-liquid-electron-crystal) concept, the mobility of Cu atoms in the crystal structure leads to decreased thermal conductivity without affecting the electrical conductivity to the same extent,[14] e.g. in Cu_2Se or $CuCrSe_2$.[15] The incorporation of magnetic ions like Mn and Fe promises changes in oxidation states and mixed valency, which may have an intriguing influence on thermoelectric properties and stability. So far, single crystal structures of Mn or Fe substitution variants of pavonite-type $Cu_{1.7}Bi_{4.7}Se_8$ have not been reported.
In line with the key topic of energy materials, oxonitridosilicates are highly important in the field of luminescent materials for phosphor-converted LEDs.[16] Accurate structural data are useful for comprehension of luminescence properties due to their dependence on the coordination sphere, ligand field and symmetry of the activator site. Syntheses of these compuonds often involve extreme reaction conditions, which can lead to inhomogeneous and microcrystalline samples.

Experimental details and results

Prior to the beamtime, samples were investigated by means of TEM in combination with EDX in order to make sure to select interesting crystallites, i. e. finding new compounds. The respective crystallites were mounted on carbon-film-coated TEM finder grids. The latter were fixed on glass fibers in a way that the crystal of choice (or parts of it) was best accessible by the beam. At beamline ID11 (EH3), we used an optical telescope to align the crystallites in the beam and performed fluorescence scans for final centering. For the experiments with a microfocused beam, the energy was kept at 30 keV to assure minimal absorption for the investigated compounds and maximal brilliance of the beam. The following samples were examined:

a) La oxonitridophosphate

A dataset of a new La containing oxonitridophosphate was collected. The compound exhibits monoclinic metrics with lattice parameters of a = 14.042(4) Å, b = 7.086(3), c = 41.41(1) Å and β = 97.70(3)°. The structure determination will be completed in the near future.

b) $Pb_2Si_5N_8$

This structure was elucidated based on the dataset from ID11: space group $Pmn2_1$ with lattice parameters a = 5.774(1) Å, b = 6.837(1) and c = 9.350(1) Å (R_{int} = 0.051, R1(obs) = 0.023, cf. Fig. 1). The compound crytallizes similarly to $M_2Si_5N_8$ (M = Sr, Ba) [17], but differs with respect to the distribution of Pb–N distances. The interaction between these atoms is less ionic than in common nitridosilicates. The most remarkable feature is the significant homonuclear bond in pairs of Pb atoms. The Pb-Pb distance of 3.19 Å is rather typical for plumbanes, diplumbenes or Zintl phases.

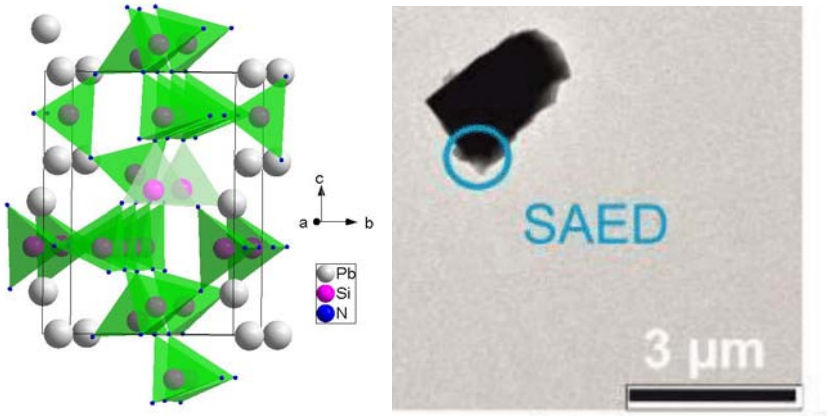

Figure 1: Crystal structure and image of a selcted crystal of $Pb_2Si_5N_8$.

c) $U_{0.53}Sr_{1.21}Si_5N_8$

This structure was also elucidated based on a dataset from ID11: space group $Pmn2_1$ with lattice parameters a = 17.1295(3) Å, b = 6.7890(2) and c = 9.3079(2) Å (R_{int} = 0.083, R1(obs) = 0.088). It corresponds to a superstructure of the $Sr_2Si_5N_8$ type, from which it was synthesized by ion exchange.

d) $SrBe_8N_6$

Data collected during this beamtime revealed a new compound in the system Sr/Be/N. The crystal is probably twinned, the final structure refinement will be completed in the near future. The compound is characterized by BeN_4 tetrahedra and some Be atoms that are coordinated in trigonal planar fashion.

e) $LiSr_3P_{10}N_{19}$

This compound (Fig. 2) crystallizes in space group *Pnma* with lattice parameters a = 13.851(3) Å, b = 8.381(2) and c = 13.174(3) Å (R_{int} = 0.0479, R1(obs) = 0.0365). It contains a rather complex network of PN_4-tetrahedra, which form channels. These are filled with columns of Sr atoms in their centers and Li atoms besides them.

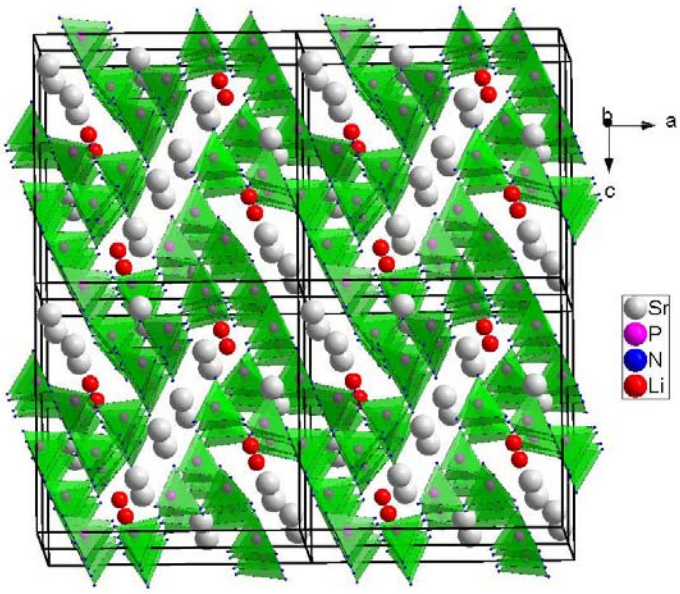

Figure 2: Crystal structure pf $LiSr_3P_{10}N_{19}$.

In addition, precise temperature-dependent data up to 600 °C from larger crystals (50 – 100 µm) and powder samples were collected using the diffractometer in EH1. These crystals were fixed on glass fibers mounted on metal pins. The powder samples were filled into silica capillaries under argon. The following samples were examined:

f) $Mn_{0.85}Bi_{4.1}Te_7$ and $Mn_{0.81}Bi_{6.13}Te_{10}$

Temperature-dependent PXRD data for both phases were obtained. The $GeBi_4Te_7$ and $GeBi_6Te_{10}$-type structures showed no changes except thermal expansion up to ca. 210 °C. At this temperature, both phases start to decompose to phases with Bi_2Te_3 structure type and a $MnTe_2$-like phase. The decomposition is complete at 270 °C for $Mn_{0.85}Bi_{4.1}Te_7$ and at 295 °C for $Mn_{0.81}Bi_{6.13}Te_{10}$.

g) $Cu_{1.5}Mn_{0.5}Bi_{4.5}Se_8$ and $Cu_{1.3}Fe_{0.4}Bi_{4.7}Se_8$

High-quality temperature-dependent single-crystal data of $Cu_{1.3}Fe_{0.4}Bi_{4.7}Se_8$ (Fig. 3) up to resolutions > 0.6 Å were obtained. The compound crystallizes in the ^{3}P-pavonite-type structure (space group *C*2/*m*, a = 14.773 Å, b = 4.1564 Å, c = 13.572 Å, β = 115.51°, V = 752.1 Å^3, R1(obs) = 0.0654 at RT). The lattice parameters increase with temperature in a linear fashion; there is no phase transition. The Se split position [9] becomes smeared-out at higher temperatures and the coordination polyhedra become more regular. Anharmonic displacement parameters are currently being evaluated.

Single-crystal data of $Cu_{1.5}Mn_{0.4}Bi_{4.5}Se_8$ were obtained near RT, but the crystal was destroyed during heating. The structure (space group *C*2/*m*, a = 13. 647 Å, b = 4.1392 Å, c = 14.783 Å, β = 115.76°, V = 752.0 Å^3, R1(obs) = 0.0524) is similar to that of the pristine material, but exhibits a reduced cell volume.[9] Data at higher temperatures were obtained from an aggregate of several crystals, which requires more extensive evaluation.

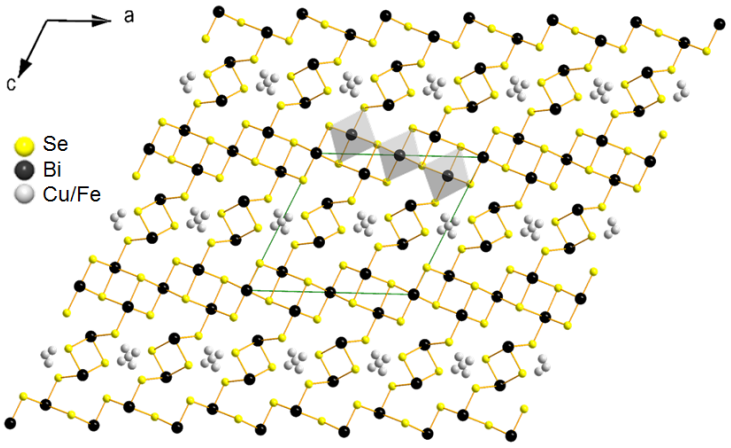

Figure 3: Crystal structure of $Cu_{1.3}Fe_{0.4}Bi_{4.7}Se_8$.

h) Cu_5FeS_3Se and $Cu_4FeS_{2.2}Se_{1.6}$

Temperature-dependent PXRD data of Cu_5FeS_3Se were obtained between 115 °C – 640 °C – 115 °C (heating and cooling) and show that the superstructure observed at room temperature does not exist at temperatures above 115 °C. The intermediate-temperature (IT) phase of Cu_5FeS_4 [18] is stable up to ~200 °C during heating and forms again at ~220 °C upon cooling, whereas its high-temperature (HT) phase is stable from 200 °C to at least 640 °C. The metastable phase $Cu_4FeS_{2.2}Se_{1.6}$ (corresponding to the modulated HT phase of Cu_5FeS_4 [18]) is observed at least up to 640 °C; however upon slow cooling the IT phase occurs below ~240°C.

Outlook

The combination of TEM and microfocus synchrotron diffraction is an excellent tool for challenging structure determinations where electron diffraction or conventional X-ray and synchrotron diffraction alone are not sufficient. A broad range of different structures were elucidated and intriguing new structural features like covalent Pb-Pb interactions were discovered. The first publications are already written, and more papers will follow soon. These results motivate us to continue structure determination by combination of TEM and microfocus synchrotron data and develop futher more specialized applications, e.g. by combination with resonant scattering. The structural characterization may further be enhanced by the use of a heat source or cooling unit. This way, the analysis phase transitions, metastable phases, etc. would be feasible.

References

[1] Y. Ni, Z. Zhang, I- C. Nlebedim, R. L. Hadimani, D. C. Jiles, *IEEE Trans. Magn.* **2015**, *51*, 1–4.
[2] J. Choi, S. Choi, J. Choi, Y. Park, H.-M. Park, H.-W. Lee, B.-C. Woo, S. Cho, *Phys. Status Solidi B* **2004**, *241*, 1541–1544.
[3] S. V. Eremeev, M. M. Otrokov, E. V. Chulkov *Nano Lett.* **2018**, *18*, 6521.
[4] D. S. Lee, T.-H. Kim, C.-H. Park, C.-Y. Chung, Y. S. Lim, W.-S. Seo, H.-H. Park, *Cryst. Eng. Comm*. **2013,** *15*, 5532.
[5] D. Durach, L. Neudert, P. J. Schmidt, O. Oeckler, W. Schnick, *Chem. Mater.* **2015**, *27*, 4832.
[6] F. Fahrnbauer, T. Rosenthal, T. Schmutzler, G. Wagner, G. B. M. Vaughan, J. P. Wright, O. Oeckler, *Angew. Chem. Int. Ed.* **2015**, *54*, 10020.
[7] M. S. Jagadeesh, H. M. Nagarathna, P. A. Montano, M. S. Seehra, *Phys. Rev. B* **1981**, *23*, 2350.
[8] V. P. Kumar, T. Barbier, P. Lemoine, B. Raveau, V. Nassif, E. Guilmeau, *Dalton Trans.* **2017**, *46*, 2174.
[9] E. Makovicky, I. Sotofte, S. Karup-Moller, *Z. Kristallogr.* **2006**, *221*, 122.
[10] J.-Y. Hwang, M.-W. Oh, K. H. Lee, S. W. Kim, *J. Mater. Chem. C* **2015**, *3*, 11271.
[11] J.-Y. Hwang, H. Mun, J. Y. Cho, S. S. Yang, K. H. Lee, S. W. Kim, *J. Nanomater.* **2013**, *3*, 1.
[12] J. Y. Cho, H. Mun, B. Ryu, S. I. Kim, S. Hwang, J. W. Roh, D. J. Yang, W. H. Shin, S. M. Lee, S.-M. Choi, D. J. Kang, S. W. Kim, K. H. Lee, *J. Mater. Chem. A* **2013**, *34*, 9768.
[13] J.-Y. Hwang, H. A. Mun, S. I. Kim, K. M. Lee, J. Kim, S. W. Kim, *Inorg. Chem.* **2014**, *53*. 12732.
[14] H. Liu, X. Shi, F. Xu, L. Zhang, W. Zhang, L. Chen, Q. Li, C. Uher, T. Day, G. J. Snyder, *Nat. Mater.* **2012**, *11*, 422.
[15] Y. Yan, L. Guo, Z. Zhang, X. Lu, K. Peng, W. Yao, J. Dai, G. Wang, X. Zhou, *Scr. Mater.* **2017**, *127*, 127.
[16] M. Zeuner, S. Pagano, W. Schnick, *Angew. Chem. Int. Ed.* **2011**, *50*, 7754.
[17] T. Schlieper, W. Milius, W. Schnick, *Z. Anorg. Allg. Chem.* **1995**, *621*, 1380.
[18] N. Morimoto, *Acta Crystallogr.* **1964**, *17*, 351.